THE EXTENDED BRANCH-ARROW MODEL OF THE FORMATION OF RETINO-TECTAL CONNECTIONS

Kenneth J. Overton
and
Michael A. Arbib

COINS Technical Report 82-08

(February 1982)

This is a revised version of COINS Technical Report 81-14.

The research reported in this paper was supported in part by grant NS14971-03 from the National Institutes of Health.

Submitted to Biological Cybernetics

THE EXTENDED BRANCH-ARROW MODEL OF THE FORMATION OF RETINO-TECTAL CONNECTIONS

Kenneth J. Overton and Michael A. Arbib
Center for Systems Neuroscience,
Computer and Information Science
University of Massachusetts
Amherst, MA 01003

(February 1982)

Abstract

This paper presents XBAM (the Extended Branch-Arrow Model), a new model of the development of the retino-tectal topographic mapping as observed in frog, toad, and goldfish visual systems. The updating process employed by XBAM is distributed in nature and depends upon interactions between branches of retinal fibers, the branches and the boundaries of the tectum and grafts, and the branches and the tectal surface. Results of computer simulation of the model are related to experimental data obtained from tectal and retinal graft and lesion studies, and comparisons are also made with other models.

I. Introduction

Many experiments study the development of the topographic mapping between the retina and tectum of various lower vertebrates. Goldfish, frog, and toad visual systems have generally been the targets of these studies. In these animals the fibers from each retina project to the contralateral tectum. Early behavioral

studies (Sperry 1943, 1944, 1945, Gaze 1959, Maturana et al. 1959) showed that the retinal projections of these animals would regrow to map in an orderly way after surgical interruption. With the development of electrophysiological recording techniques, investigators have been able to better understand the details of the mapping (Gaze et al. 1963, 1965, 1970, 1974, Jacobson 1965). Stimuli in the superior section of the visual field project to the medial section of the contralateral tectum while those in the inferior field project to the lateral side. Similarly, stimuli in the nasal portion of the visual field project to the rostral end and temporal stimuli to the caudal end of the contralateral tectum (see Figure 1). As the body of experimental data has grown, numerous models of the process by which the mapping is formed have been proposed. The models can be divided into two general classes: those subscribing to the idea of a point-to-point chemoaffinity between the retinal and tectal cells and those using the idea of systems-matching.

Figure 1

Sperry (1944, 1945, 1963) first proposed the idea of chemoaffinity between the layers of cells. Under this hypothesis, each retinal cell is uniquely labeled according to its position on the retina. The tectal surface is considered to be labeled in a similar manner and organization of the map is the result of each retinal cell axon seeking the point on the tectum which matches its own retinal label. The Marker Induction model of Willshaw and von der Malsburg (1979) may be viewed as a sophisticated development of this idea in that the tectal "addresses" are not prespecified, but rather develop as a result of the interactions among retinal fibers.

In system matching models, the information available to the retinal fibers is considerably less specific. Retinal fibers do not seek a particular point on the tectum, but rather seek a neighborhood where the interactions with the surrounding

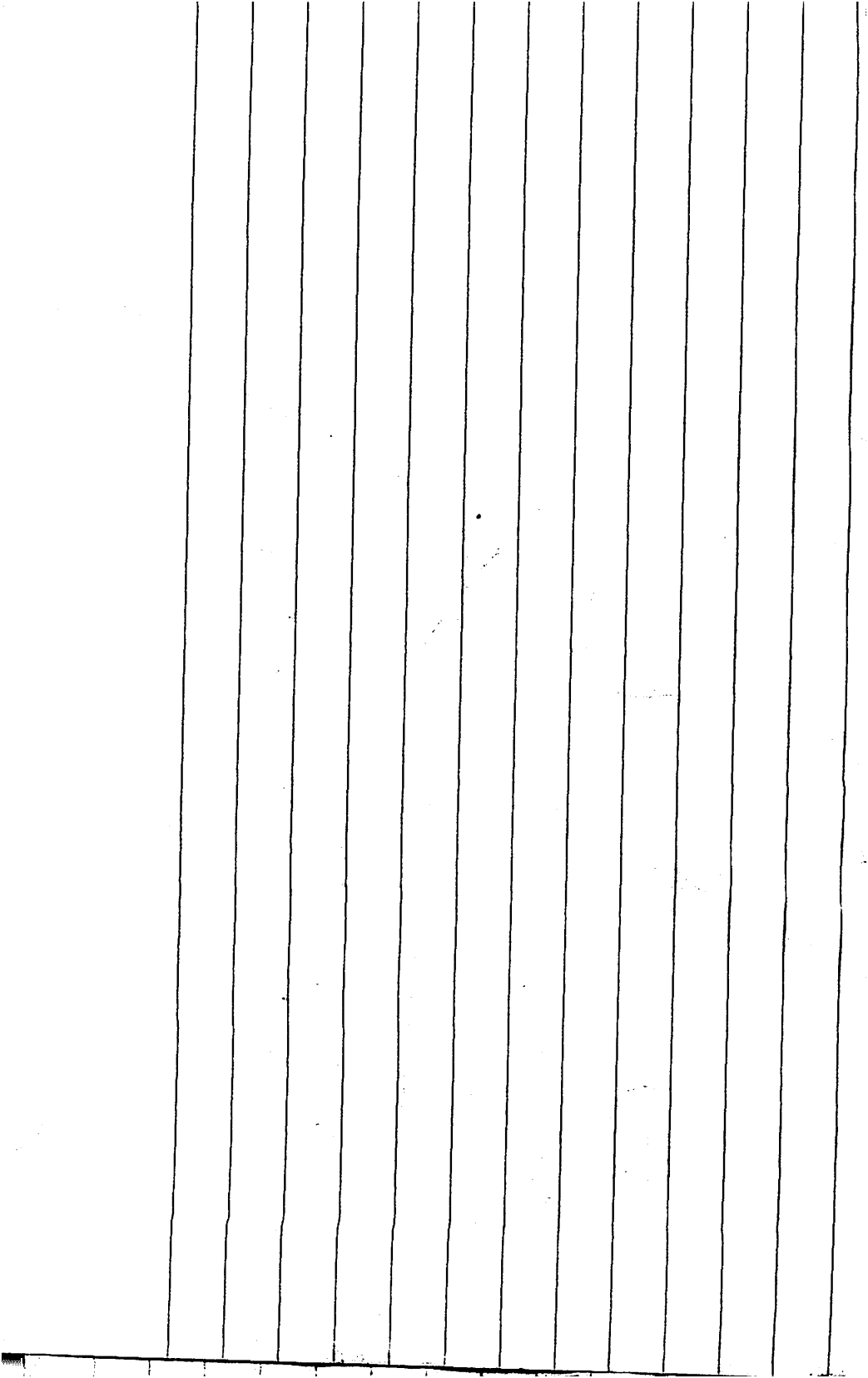

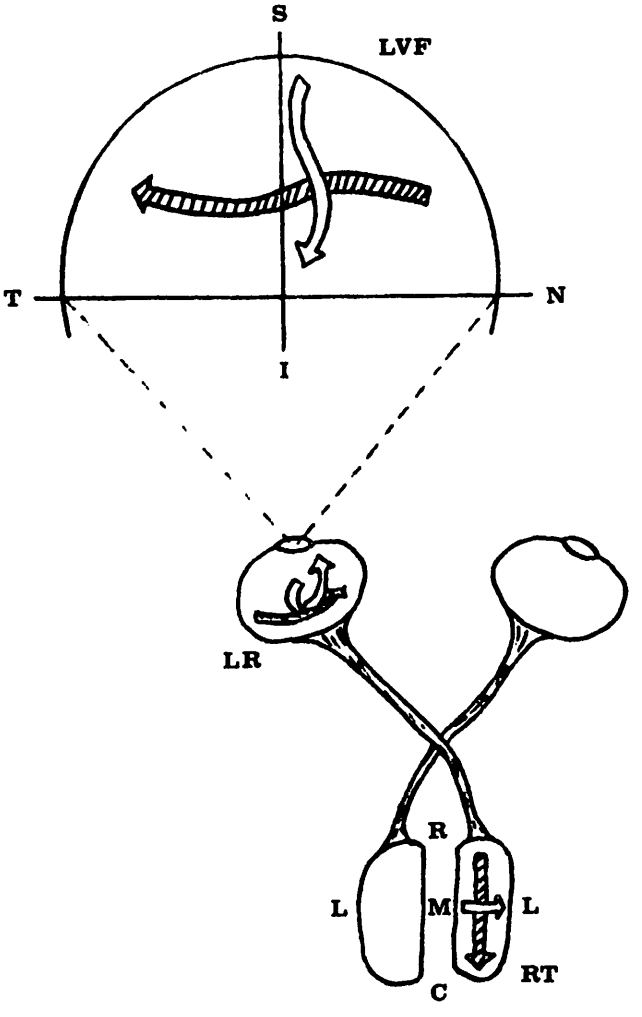

Figure 1. Schematic of the frog visual system. Fibres from the retina project onto the contralateral tectum. Tectum: R - Rostral, C - Caudal, M - Medial, L - Lateral. Visual Field: N - Nasal, T - Temporal, S - Superior, I - Inferior.

fibers match the activity on the retina. The Arrow model proposed by Hope et al. (1976) may be placed in this class.

While the Marker Induction and Arrow models employ different underlying assumptions as to the amount and type of information required by the organization process, they both exhibit many aspects of the experimental data. The model presented in this paper combines new ideas with concepts from both of these approaches to produce a hybrid model which explains a wide body of experiments.

II. An Overview of the Model

We present an overview of four models of increasing complexity: the Arrow Model, our first extension of it (Overton and Arbib, 1982), the Branch Arrow Model (BAM) which is still a systems matching model, the Marker Induction Model, and then the Extended Branch Arrow Model (XBAM) which incorporates both systems matching and certain chemoaffinity features. The mathematical specification of the models is provided in the Appendix.

In the Arrow Model, the tectum is modelled as a discrete grid with retinal fibers allowed to terminate only at the intersections of the grid lines, called tectal sites. Each iteration of the sorting process may assume one of the two forms: switching interaction or random walking.

Switching interaction (see Appendix A) is, essentially, a two-dimensional "bubble-sort" -- retinal fibers with adjacent positions on the retina will switch the position of their terminations if the relative positions on tectum differs from relative positions on the retina. Note, then, that the model uses relative position, not "absolute addressing". Switching interaction is applied to all fibers in such a way that no fiber interacts with more than one other fiber during any iteration. Repeated application of this process produces an ordered mapping from

one in which the initial positions were originally randomly assigned.

Using this mechanism alone, there is no way for fibers to move into previously unoccupied termination sites, an ability required in the case of a hemiretina projecting onto a complete tectum. In order to circumvent this problem, the fibers are periodically allowed to take random steps.

During an iteration of random walking, a site adjacent to each fiber is chosen at random. If the site is empty, the fiber moves to occupy that location. If the site is occupied or one or more other fibers are trying to move into it the fiber retains its original location. One iteration of random walking consists of applying this process to each fiber on the tectum. The updated positions form the initial state for the succeeding iteration.

The overall sorting method in the Arrow Model involves the use of switching interaction and random walking. These are combined by alternating which method is used during successive iterations. The majority of the iterations employ the switching interaction while a few, spaced at predetermined intervals, employ the random walk. This use of the random walk allows the fibers to disperse to all parts of the tectum while the switching interaction provides a degree of ordering in the mapping.

Our Branch-Arrow Model (BAM) redefines the Arrow model in several ways. In the Arrow Model, retinal fibers must terminate at discrete points on a grid; in BAM, retinal fibers form several branches as they reach the tectal surface which is now modelled as a continuum rather than a grid. The termination of each branch is surrounded by a circle which represents its area of interaction with other branches (see Figure 2). The circle is meant to model the area of synaptic efficacy of the branch. Further, each branch explicitly interacts with the tectal and graft boundaries. These changes also dictate that the neighborhood interaction rules be modified. In our model the neighborhood interaction process is applied to each

branch so that the actual position of a fiber as a whole is determined implicitly by the locations of its branches. The resultant model, BAM, seems to more closely resemble the physiology of fiber movement. The reader is referred to Appendix B for a complete development of BAM. However, there is a small number of experiments which cannot be accounted for by either the Arrow Model or BAM. The Extended Branch-Arrow Model, XBAM, adds fiber-surface interaction to the Branch-Arrow model.

Figure 2

In (X)BAM, then, the movement of a retinal fiber is determined by the overall trend of the movements of its individual branches. Rather than the discrete 'pick a neighbor, and switch if appropriate' of the Arrow Model, (X)BAM has the move of a branch determined as a vector sum of the 'nudges' applied by all other branches within its circle of interaction. The direction for each 'nudge' is very similar to that given by the interchange rule used in the Arrow Model. The main difference lies in the stipultation that if the somas are separated by a distance greater than a specified value, the direction of the influence is chosen at random. The authors feel that retinal cells may communicate in a meaningful way only if their somas are within a certain distance, e.g. if their receptive fields overlap. Thus if the cells are separated by a great distance, no communication is possible. When the somas of two interacting branches are within the distance allowing meaningful communication, the direction is chosen as in the Arrow Model. When the branch terminations are oriented on the tectum the same relative to some axis system as are the somas on the retina, relative to the corresponding axis system, the influence tends to force the branches apart. If, however, the branch positions are reversed compared to the relative soma locations on the retina, the influence tends to force the branches to move past one another, i.e. interchange positions. In the case where both of the interacting branches in question belong to the same fiber, the

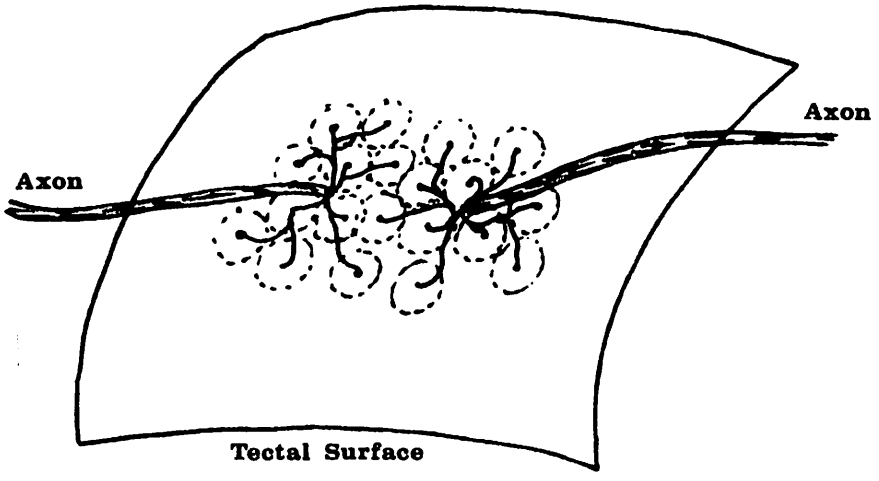

Figure 2. Axonal arborization: retinal fibre termination configuration used in BAM and XBAM.

influence felt by one from the other always tends to force the branches apart thereby attempting the maximize the area of the tectum covered by a fiber. The second component of the physical influence involves the interaction between the branches and the tectal and graft boundaries.

Tectal and graft edges are physical discontinuities in the surface of the tectum. We thus hypothesize that it is more difficult for a branch to migrate across such a boundary than to move across an unobstructed surface. In addition, we propose that communication between fibers separated by such a boundary is more difficult than between fibers on an unobstructed surface. Thus, in (X)BAM, we model the influence of boundaries as restrictions on the movements of the branches.

As we have verified in computer simulations reported elsewhere (Overton and Arbib, 1982), BAM, using the principles of system matching, accounts for a great deal of the experimental data. Relative retinal and tectal orientation information is sufficient to produce behavior similar to most of the experimental results when utilized by neighborhood and boundary interaction mechanisms. If the effect of retinal separation on the ability of two retinal cells to communicate is investigated, degraded behavior results. Restricting the distance allowing a meaningful exchange to a fraction of the retinal expanse results in a locally continuous yet globally discontinuous mapping. However, we found that BAM cannot accurately produce the graft rotation and translocation behavior seen experimentally. The systems matching approach lacks specific information differentiating individual tectal locations and the ability for information to be shared over distances which are large relative to the neighborhood interaction. Unlike the system matching ideas, point-to-point chemoaffinity provides specific information describing every point on the two surfaces.

We now briefly discuss the Marker Induction model of Willshaw and von der Malsburg as a sophisticated representitive of the point-to-point chemoaffinity

approach. The Marker Induction model (Willshaw 1979) involves the specification of the tectal surface by actions of the incoming fibers with the specificity determining, and determined by, the differential growth of synapses between retinal fibers and tectal cells. The retinal surface is posited to possess concentration gradients of a number of transportable substances, with at least one for each spatial dimension. Each retinal cell continually absorbs each of these substances at rates proportional to the concentrations at the cell's location. Thus the cell's retinal location can be uniquely determined by the vector of concentrations. The substances are moved to the synapses by axonal transport where they are injected into the postsynaptic cells at a rate proportional to their concentration and the strength of the synapse.

Each synapse between a retinal fiber and a tectal cell is described by two quantities: strength and fitness. The strength is an indication of the rate of transfer of the substances between pre- and postsynaptic cells. The fitness describes the similarity between the substance concentration vectors of the pre- and postsynaptic cells. The actual interaction between synapses is governed by a set of three rules:

1. The strength of a synapse is proportional to its fitness. The greater the fitness, i.e. the closer the concentration vectors, the greater the strength.
2. The sum of the strengths of all of the synapses of each presynaptic cell is stipulated to be fixed. This accomplishes two things: first, no synapse can grow without bound; and second, this provides competition between synapses of the same cell. If a particular synapse is to be strengthened, the other synapses must be weakend accordingly.
3. Finally, each axon forms new branches in the neighborhood of existing ones and branches with synapses whose strengths are below a minimum value are removed.

The above assumptions and rules provide a method for producing locally continuous maps. However, since the model contains no specific orientation information, there is no preference for one particular final organization over another. In computer simulations of the one dimensional version of this model, an initially random organization resulted in piecewise continuous maps with no particular global organization -- this is similar to the results we report for BAM in the next section (Experiment I). Willshaw and von der Malsburg provide orientation information by giving the initial map some order. This is accomplished by placing the presynaptic fiber terminations in sections of the tectum which approximate the desired final locations. With this, the model is able to produce mapping behavior consistent with experimental data from both regeneration and developmental experiments.

It is our opinion that both the system matching and chemoaffinity approaches have their merits. We now present a hybridization of these two ideas which is posited to have available information which is more specific than that used by the system matching models yet not as specific as that used by the chemoaffinity models. Our Extended Branch-Arrow Model (XBAM) adds a branch-surface interaction mechanism to the neighborhood and boundary interaction mechanisms of BAM. In the Arrow Model, each fiber would interact with at most one of its eight adjacent sites at each iteration. Switching interaction alone was sufficient to account for much of the experimental evidence but random stepping had to be added to account for the expansion results (Schmidt 1978a, 1978b). Even with this addition, the Arrow Model cannot account for the small class of graft translocation experiments (Hope 1976). In addition, when the distance on the retina allowing an effective exchange of information is reduced from the entire retinal expanse to a fraction of that distance, the global behavior degrades markedly. By contrast, the XBAM model is able to account for essentially all of the significant experimental results.

A fiber interacts with the surface of the tectum by way of its branches. Each branch of a fiber is thought to be marked in some manner according to the retinal position of its soma. The marker need not be an indicator of its exact position but rather a marker encoding its general location, e.g. the position should be accurate to within plus or minus the distance allowing effective retinal communication. That is, the marker here is to be considered in the sense of a general position indicator as opposed to a point to point chemoaffinity. The tectal surface is also posited to be marked in a similar manner. Each of the branches sample the marker on the tectal surface. The surface influence contains a weight which is proportional to the difference between the retinal and tectal labels. For a detailed discussion of the model the reader is referred to Appendix C.

III. Experiments

In (Overton and Arbib, 1982), we report a series of experiments on the BAM model. Of these, we simply present one on the effect of retinal 'communication distance'. We then turn to a series of experimens on XBAM.

The results presented below were obtained through computer simulation of a one-dimensional retina/tectum pair containing 40 fibers, each with 4 branches. A one-dimensional simulation was utilized due to the amount of computation required. (A sample set of simulations of two-dimensional arrangements have been performed and the results yield concordant behavior.) In the figures, the one-dimensional tectal surface is represented along the horizontal side of the display. Similarly, the visual field (or retina) appears along the vertical axis. Each horizontal row of symbols represents one fiber with each symbol marking the position of the termination of an individual branch of the fiber. Thus for each branch of each fiber, the position in the visual field of the stimulus exciting the fiber, and thus

the retinal location of the branch's soma is indicated by the height of the row on which the symbol appears. The position of the branch on the tectum is indicated by the horizontal position along the row. Further, the lower end of the visual field display maps to the leftmost end of the tectum and the upper end of the visual field display maps to the rightmost end of the tectal representation. Thus a normal mapping is depicted by a diagonal line of symbols from the lower left corner of the display to the upper right. The physiological data are inherently two dimensional. To compare the simulation results with these data, equate the vertical axis of the simulation display in Figure 3a with the bar, V_t, in Figure 3b and the horizontal axis with bar L_t in 3b. The left end of the tectal representation corresponds to the lower, rostral, end of the bar in the upper half of Figure 3b while the lower end of the retinal representation corresponds to the right, nasal, end of the bar in the lower half of 3b.

Figure 3

Experiment I.

The purpose of this experiment was to study the effects of varying the maximum distance allowing effective communication between cells on the retina. The initial distribution of branch terminations on the tectum was random as illustrated in Figure 3a. Figure 4a shows the organization resulting after 8000 iterations with the radius set to allow effective communication over roughly two thirds of the retina. That is, if two cells are separated by a distance greater than two thirds of the total retinal expanse, then they cannot meaningfully communicate. Thus branches at opposite ends of the retina interact at random. The resulting configuration shows two organized maps on the tectum. The simulation results depicted in Figure 4b show the state after 8000 iterations with the radius set to roughly one half of the total retinal size. In this case, three maps are produced.

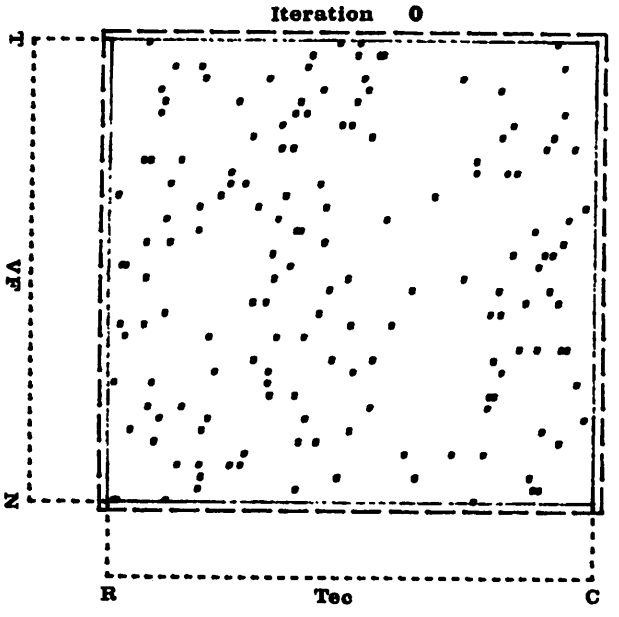

(a)

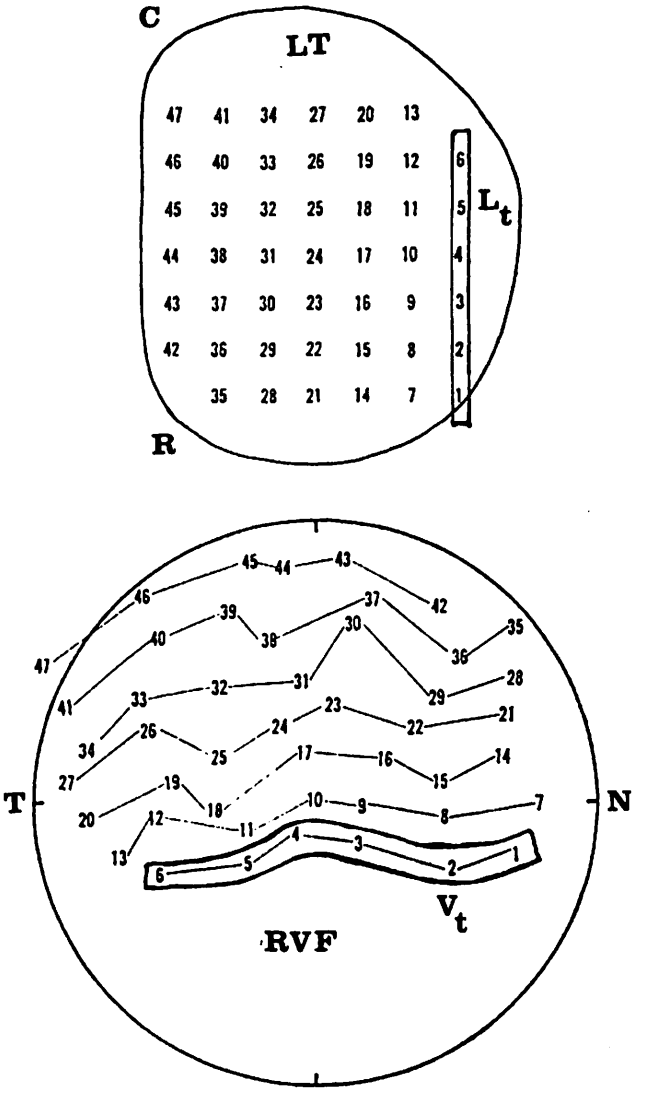

(b)

Figure 3. (a) The initial distribution of branch terminations for the BAM simulation. 40 fibres with 4 branches/fibre.

(b) The projection of right visual field onto the left tectum in a normal animal (Gaze 1974). L_t: a single line of electrode positions which is analogous to the one-dimensional tectum in BAM and XBAM. V_t: the corresponding single row of points in the visual field which excite the tectal positions -- analogous to the vertical axis of the BAM/XBAM display.

Figure 4c shows the map resulting when the distance is reduced to one fifth of the retinal size. Again, several organized pieces are seen. With the radius reduced to one tenth, the configuration in Figure 4d results. The map contains many small pockets of organization yet lacks global organization. The final subfigure, Figure 4e, shows the resulting map when the retinal interaction distance is reduced to approximately one twentieth of the total retinal expanse. Some areas of organization can be seen, although no global organization is apparent.

Figure 4

This experiment demonstrates that as the distance on the retina within which an effective exchange of information can take place is reduced, the amount of global organization is also reduced. The Arrow Model is essentially the discrete analog of the Branch-Arrow Model when the retinal interaction distance in the latter is equal to the width of the retina. It seems to us that the physiology of the visual systems being studied would indicate that an assumption of effective communication between any two retinal cells regardless of their separation is questionable. Alternately, the distance should be reduced to some fraction of the total width. The exact amount is unknown. The lack of global organization which results when the distance is reduced is evidence that a local neighborhood interaction mechanism alone is insufficient to account for the organizational behavior observed in the physiological experiments. This point will be addressed in greater detail with XBAM.

With this, we now turn to the study of XBAM (see Appendix C for the formal specification of XBAM by the addition of some tectal specificity to BAM):

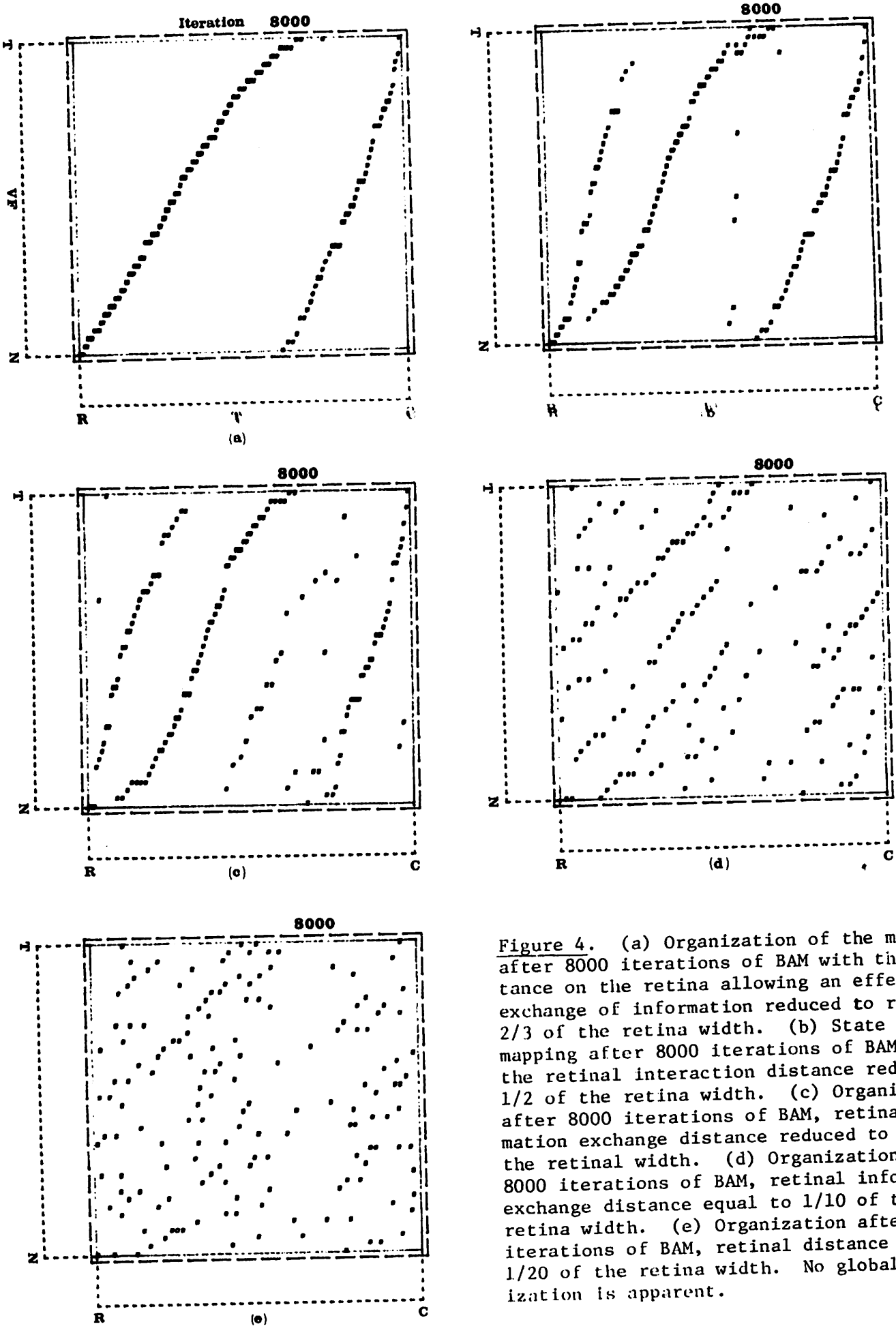

Figure 4. (a) Organization of the mapping after 8000 iterations of BAM with the distance on the retina allowing an effective exchange of information reduced to roughly 2/3 of the retina width. (b) State of the mapping after 8000 iterations of BAM with the retinal interaction distance reduced to 1/2 of the retina width. (c) Organization after 8000 iterations of BAM, retinal information exchange distance reduced to 1/5 of the retinal width. (d) Organization after 8000 iterations of BAM, retinal information exchange distance equal to 1/10 of the total retina width. (e) Organization after 8000 iterations of BAM, retinal distance equal to 1/20 of the retina width. No global organization is apparent.

Experiment II.

In this experiment, the development of the projection from a normal retina onto a normal tectum was studied for XBAM. Figure 5 illustrates the initial random positioning of the branches. Figure 6 contains the state of the mapping after 10,000 iterations of XBAM. Retinal cells were allowed to exchange information regardless of the distance between them. XBAM produced an ordered mapping.

Figures 5 and 6

We next tested the effect of reducing the distance allowing effective communication on the retina, cf. Experiment I. Figure 7 contains the mapping after 28,000 iterations of XBAM with the retinal distance reduced to roughly one half of the retina. XBAM produced a globally ordered map while BAM produced several superpositioned maps, cf. Figures 7 and 4b. The surface interaction term added enough information to allow the neighborhood and boundary mechanisms to produce a completely organized projection.

Figure 7

Experiment III.

Work has been conducted in regard to the compression of the projection onto tectum of which one half has been completely ablated. Udin (1977) and others (Sharma 1977, Yoon 1976) have studied the form of the retino-tectal projection in such a paradigm in the frog visual system. The results obtained from these experiments are generally consistent. An ordered mapping of the entire visual field is found on the intact portion of the tectum. The projection is compressed to fill the available space. The physiological results are displayed in Figure 8, from (Udin 1977).

Figure 8

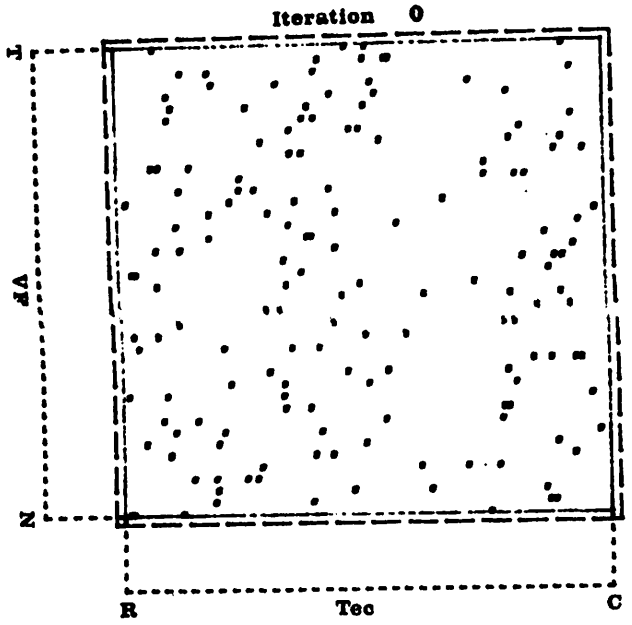

Figure 5. Initial branch distribution for the XBAM simultions. 40 fibres with 4 branches/fibre.

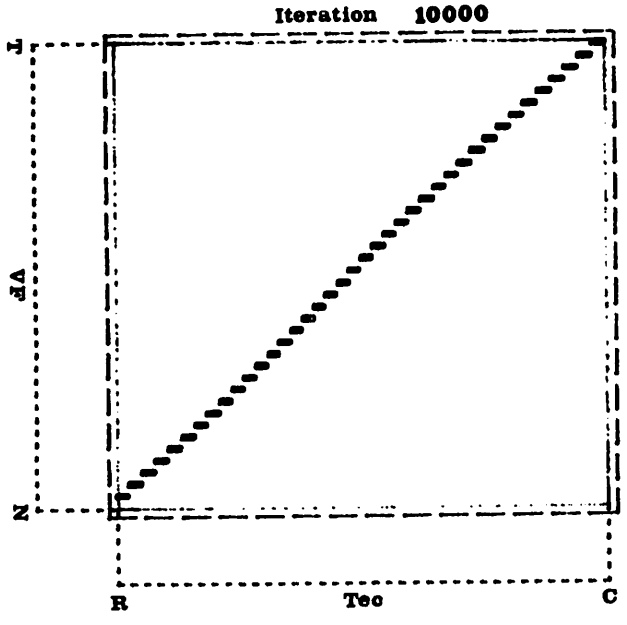

Figure 6. Mapping organization after 10,000 iterations of XBAM with the retinal distance allowing effective communication equal to the entire retina width.

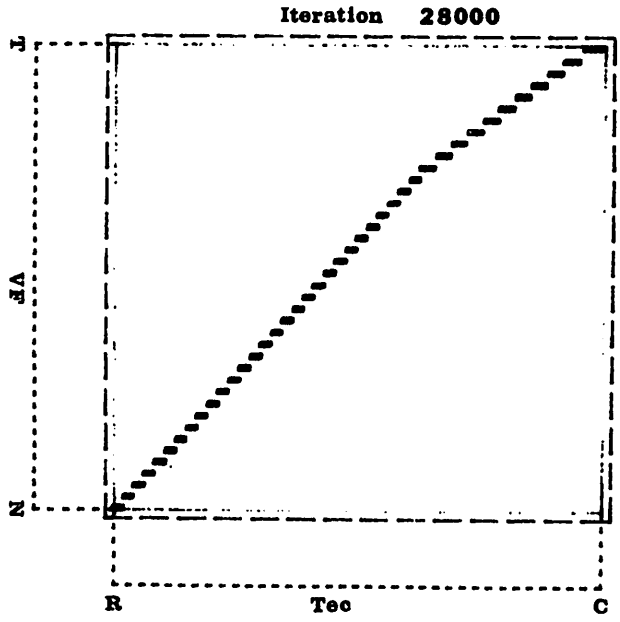

Figure 7. Projection after 28,000 iterations of XBAM with the retinal interaction distance reduced to roughly 1/2 of the retina width.

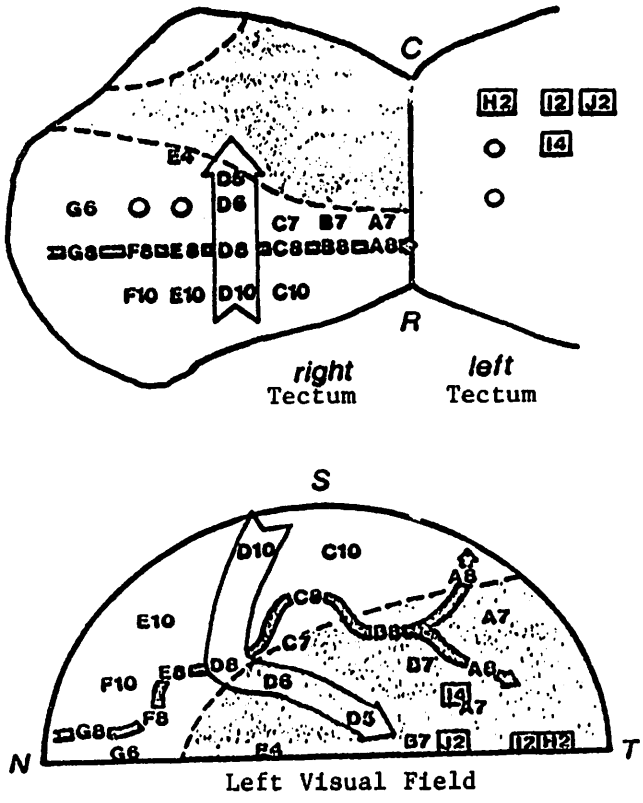

Figure 8. Physiological data from caudal 1/2 tectal ablation experiment (Udin 1977). The mapping from the entire visual field is compressed onto the remaining tectal surface.

The key features to note here are the facts that the entire visual field is represented along the dimension where only half of the original surface remains and that along the other dimension, all of the space is utilized.

This simulation experiment involved the same experimental paradigm in that the caudal half of the tectum was ablated. Figure 9 contains the results from the XBAM computer simulation. The initial termination locations were randomly distributed over the tectal surface. The surface was reduced to one half of its original size. The organization of the projection after 15,000 iterations of XBAM is shown in the figure. This map shows excellent global organization. The branches in the extreme lower left portion of the field have been forced off of the tectal surface. The magnitude of the effect is determined in part by the relative values of the weighting constants in equations (10) and (11) of Appendix B.

Figure 9

Some investigators have noticed that a mapping identical to the original mapping with the normal tectum appears first, followed by a trend toward a complete, compressed projection (Sharma 1977, Cook 1974). Horder (1977) found duplicate maps initially which later appeared compressed. He further found that if one third or less of the surface were ablated, the projection moved immediately to a compressed state. It has been posited that this initial mapping is due, in part, to the debris left on the tectum when the optic nerve is sectioned and then degenerates. The fibers which originally mapped to the rostral half of the tectum may be guided by the debris remaining from the prior mapping. Sharma (Sharma 1977) performed an experiment to test this hypothesis and found that when the fibers are forced to reinnervate a tectum previously devoid of fibers, the compressed mapping appeared with no initially uncompressed projection.

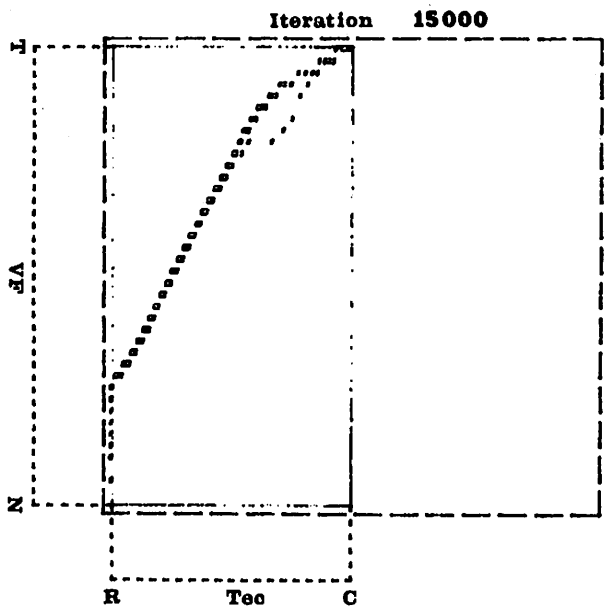

Figure 9. XBAM simulation results of a full retina mapping onto a half tectum. 15,000 iterations.

Another tectal ablation experiment involves removing 1/4 of the tectal surface and mapping the projection after regeneration. Schmidt and Easter (1978c) have performed experiments in which the medial-caudal quarter of the left tectum of the goldfish has been surgically ablated. A similar experiment designed to investigate the effect of removing part of the tectal surface was performed by Sharma (1972) and involved the ablation of a rostroventral strip on the tectal surface. An organized mapping was found compressed onto the remaining surface. The purpose of these experiments was to determin the degree to which the axes of the tectum are independent with respect to the compression of the mapping. They found that, after reinnervation of the tectum, the entire visual field was represented on the tectum. Further, the mapping was completely ordered and was compressed with respect to both axes. The compression appears to have been uniform across the tectum, that is, the fiber arbors appeared to organize in a fashion which resulted not only in an ordered representation of the visual field but also in a uniform distribution across the available tectal surface. While we cannot duplicate this paradigm due to the one dimensional nature of our simulation, we can predict the behavior of the two dimension version of the model in such a case.

Since our model tends to minimize the overlap of adjacent projection fields, as illustrated in the compression results above, and produces a continuous mapping, we would predict that the projection resulting when 1/4 of the tectal surface is removed would be uniformly compressed in all directions.

Experiment IV.

Another class of experiments involves studies of the map resulting between a hemiretina and an intact tectum (Schmidt 1978a, Horder 1971). In this case, the projection of the half of the visual field represented on the remaining hemiretina expands in an orderly manner to completely fill the available space on the tectum.

Typical results are found in Figure 10, from (Schmidt 1978b). Feldman (1975) conducted an experiment in which one eye was removed before it differentiated and the fibers from the other eye were directed to the ipsilateral tectum. He found a normal projection of the entire visual field on the ipsilateral tectum. However, some of the retinal fibers had managed to innervate the contralateral tectum to produce an expanded projection of the represented area of the visual field.

Figure 10

The simulation results for this situation are given in Figure 11. The projection of the half of the visual field represented on the remaining hemiretina expands in an orderly manner to completely fill the available space on the tectum. The XBAM simulation results for this situation are given in Figure 11. The initial locations for the branches were randomly assigned. The state after 10000 iterations shows complete organization with half of the normal number of fibers mapping onto the complete tectal surface. The mapping does not fill the entire rostral section of the tectum. This is due to a slight imbalance in the weighting constant values.

Figure 11

Experiment V.

A direct extension to the hemiretina, full tectum experiments involves studying the projection resulting when hemiretinae from different eyes are fused to form a single eye. Once the nerve connections have regenerated, the mapping is determined electrophysiologically. Gaze et al (1963, 1965) and Hunt (1973) have conducted such experiments. Their results are shown in Figure 12.

Figure 12.

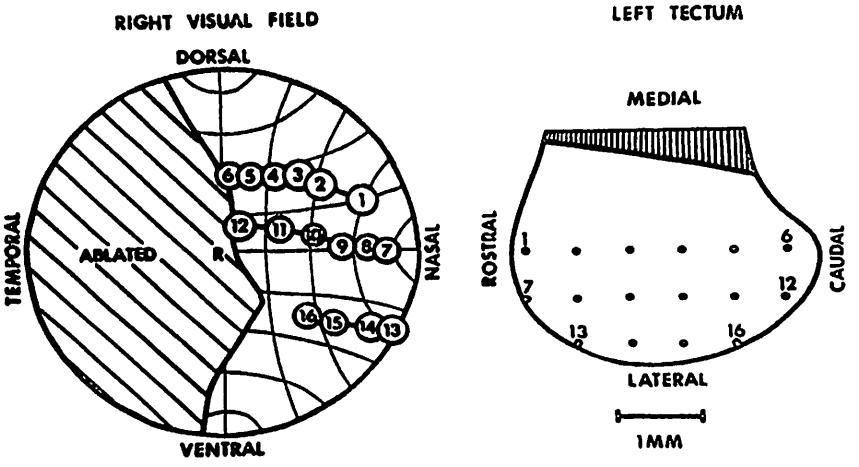

Figure 10. Physiological data from an animal in which the nasal half of the retina has been ablated. The remaining visual field is represented by an ordered projection covering all of the tectal surface (Schmidt 1978b).

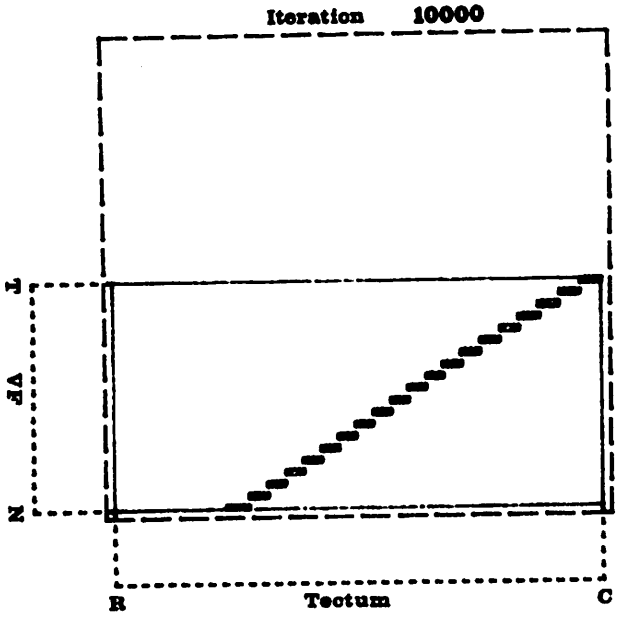

Figure 11. XBAM simulation results of a hemiretina projecting onto a full tectum, 10,000 iterations.

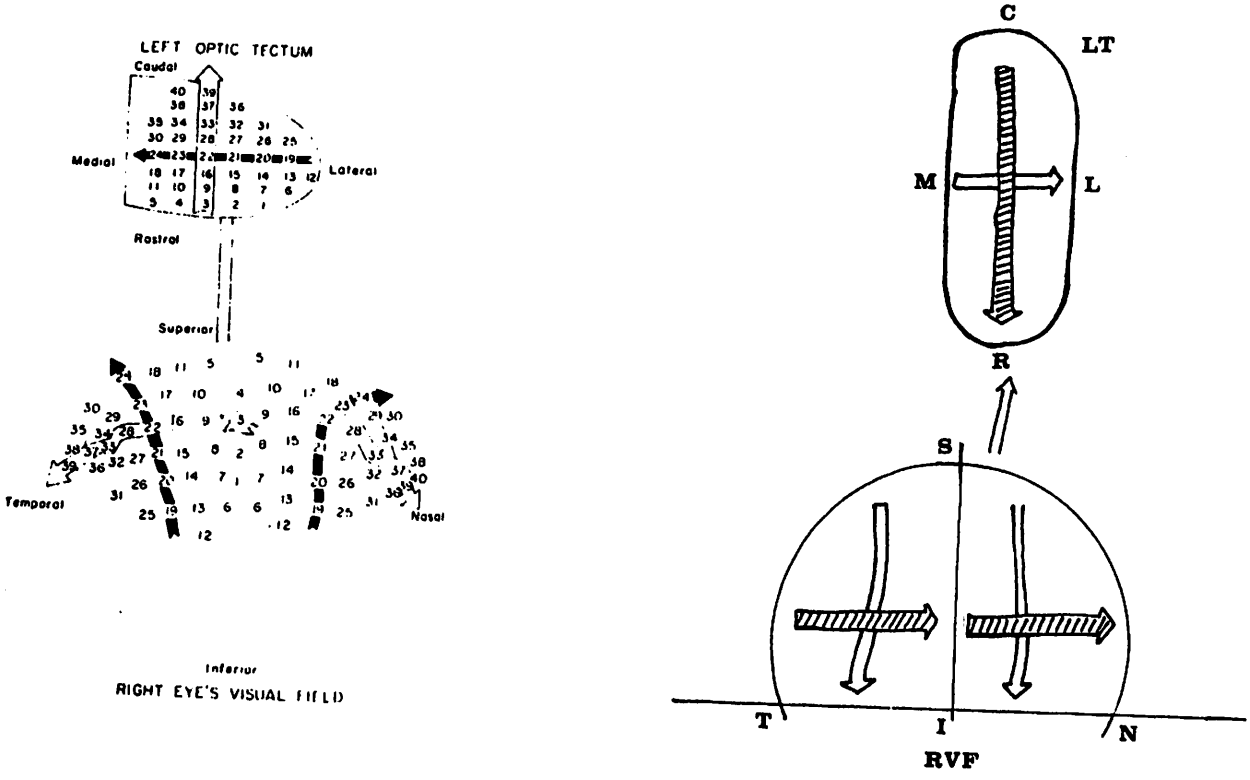

(a) (b)

Figure 12. (a) Projection of the visual field from a double-nasal compound eye onto a normal tectum (Hunt 1973). Notice that there are two overlapping projections, one from each half of the eye.

(b) Schematic of the projection resulting from a compound eye composed of the nasal hemiretinas from one eye and the temporal hemiretina from another.

In the case of Figure 12a, (Hunt 1973), the compound eye was composed of the nasal hemiretinae of two eyes with the division along the superior-inferior axis. The interesting point to note is that the projection from the two halves of the compound eye are superimposed. That is, the projection from each hemiretina expanded in an organized way to cover the entire tectal surface. The projection from one of the hemiretina is rotated 180 degrees. This is the case since one of the hemiretinae had to rotated through 180 degrees in order to create the complete eye. Figure 12b contains a schematic of the results from a compound eye composed of two temporal hemiretinae. The projections are ordered the same since neither piece required rotation when the eye was constructed.

Figures 13 and 14 contain the results from computer simulations of the XBAM when a double nasal eye maps onto the tectum. Figure 13 results from hemiretinae with their orientations retained so that the maps are oriented the same. Figure 14 was produced with the orientation of one half of the retina reversed.

Figures 13 and 14

Notice that in both cases the global organization of the field represented on each hemiretinae is maintained. However, the projection has expanded to cover most of the available tectal surface.

To this point, the experiments have focused on the mappings when there is a mismatch in the size or type (e.g. the compound eye experiments) of retinal versus tectal tissue. Another class of experiments involves the excision of a section of the tectum and its subsequent reimplantation after some form of inversion or rotation. Yoon (1975) and Sharma and Gaze (1971) have studied the projection following a 90 degree rotation of the graft tissue about the dorsoventral axis. Completely ordered projections are found both within and surrounding the graft. The projection within the graft, however, is found to be rotated in the same manner

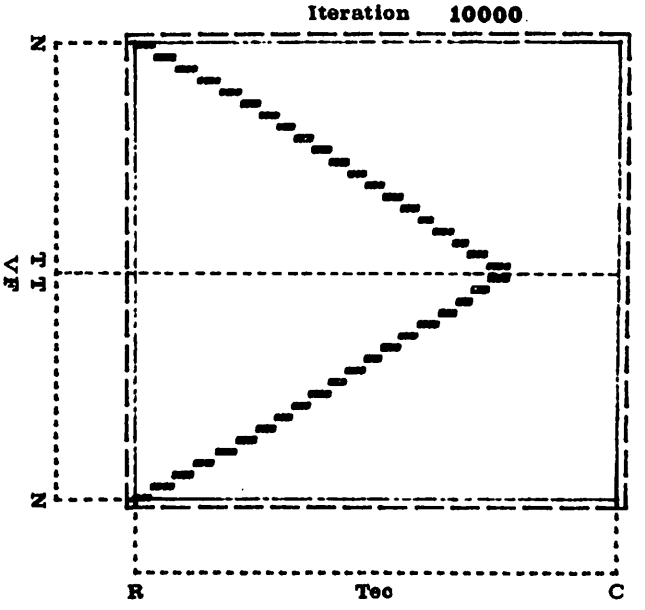

Figure 13. XBAM results of double-nasal compound eye experiment. 10,000 iterations.

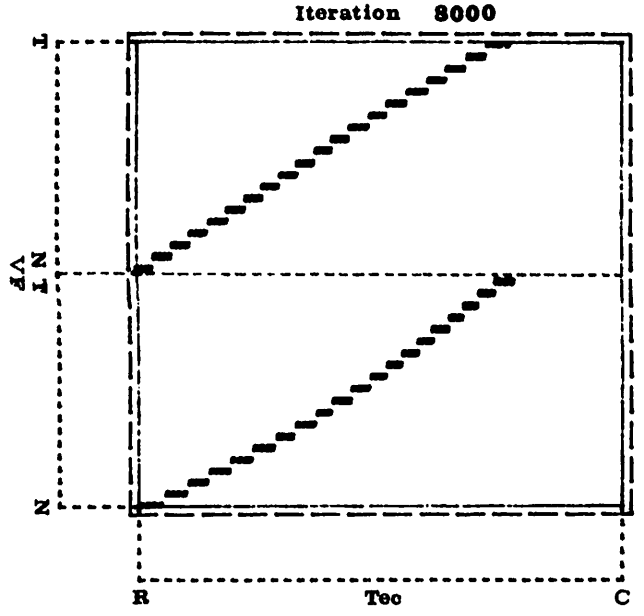

Figure 14. Results of XBAM simulation of nasal-temporal compound eye experiment. 8,000 iterations.

relative the the tectum as the graft. Figure 15, taken from (Yoon 1975) illustrates these results.

Figure 15

Several neurophysiologists (Yoon 1973, 1975, Levine 1974) have experimented with animals in which a single tectal graft has been rotated 180 degrees, again about the dorsoventral axis. Once the tectum has been reinnervated the mapping is found to be completely ordered both within and around the graft. The orientation of the map within the graft is again found to be rotated in a manner identical to the graft, see Figure 16, again from (Yoon 1975).

Figure 16

Yoon (1975) has also performed experiments in which a graft has been excised, rotated 180 degrees about the rostrocaudal axis, and reimplanted. This rotation causes the graft to retain its normal orientation along the rostrocaudal axis while having an inverted orientation along the superior-inferior axis. The resulting projection map is illustrated in Figure 17 (Yoon 1975), and shows that the map retains its normal rostrocaudal organization while the mediolateral organization within the graft is reversed. Again, the local orientation of the map follows that of the underlying tectal surface.

Figure 17

Experiment VI.

The simulation of the XBAM is one dimensional as was BAM so that the 90 degree rotation experiments cannot be performed; the two forms of the 180 degree rotation are equivalent. Figure 18a illustrates the state of organization of the branch termination locations after 8000 iterations. The initial configuration was again

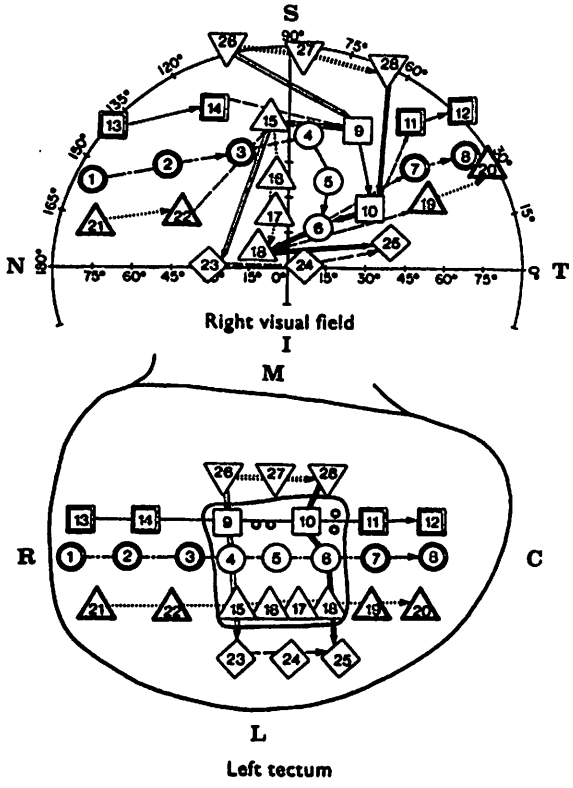

Figure 15. Mapping recorded after section of the optic nerve and 90 degree counterclockwise rotation of a graft (Yoon 1975).

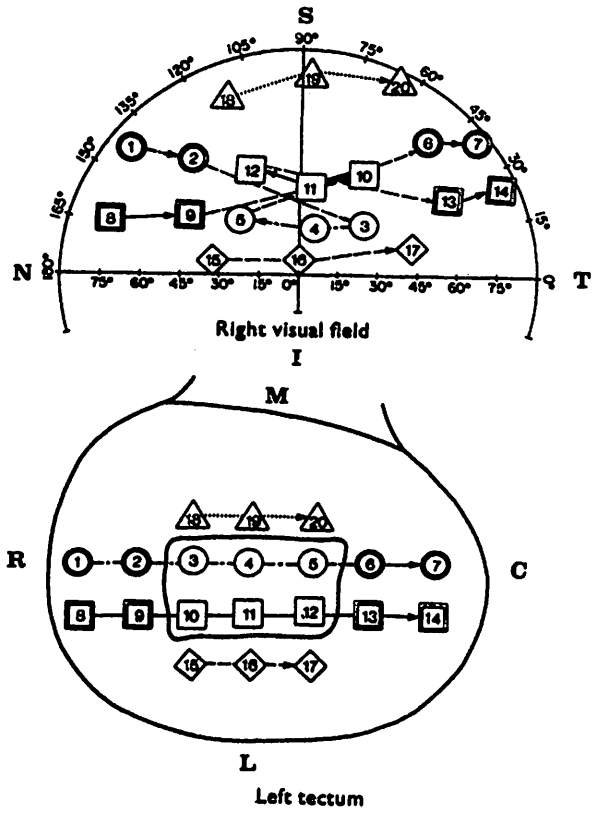

Figure 16. Visual field projection organization after optic nerve section and 180 degree rotation about the dorsoventral axis of a graft (Yoon 1975).

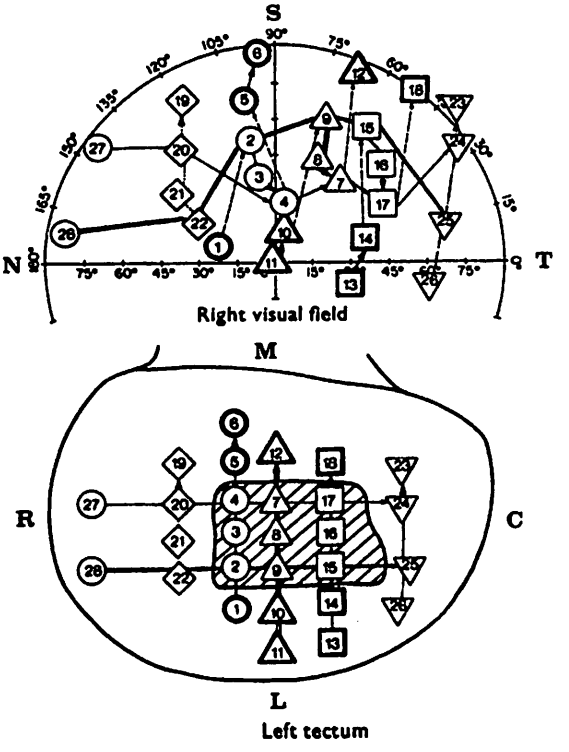

Figure 17. Projection organization after optic nerve section and graft inversion along the rostrocaudal axis (Yoon 1975).

random.

Figure 18

Notice that the most caudal section of the tectum receives information only from the temporal area in the visual field. The projection in that area is reasonably well ordered. The fibers from the nasal section of the visual field are moving toward the rostral section of the tectum. The fibers which should project onto the grafted area are trapped between those in the rostral one third of the tectum and those moving toward that end. The organization in the rostral one third of the tectum is also reasonably well ordered.

An extension to the graft rotation experiments consists of excising two pieces of tissue from the surface of the tectum and reimplanting them without rotation yet with their positions switched (Hope 1976). This is a difficult experiment to perform physiologically and the few available results are not totally consistent. In some cases, a completely normal projection is seen. This result would favor the "systems matching" theory of organization. However, different results have been obtained. In these cases the projection is ordered both within and surrounding the grafts but the grafts retain their original spatial mapping. Thus two sections of the mapping are interchanged. Since no information is available to differentiate between two tectal locations, these data support the "point-to-point chemospecificity" approach. Physiological results from such experiments are given in Figure 19, from (Hope 1976).

Figure 19

Previous experiments, cf. Overton and Arbib (1982), illustrated that the simple BAM cannot produce the behavior found in graft rotation or translation experiments. Simulation results from the translocated graft experiment appear in Figure 18b. Perfect organization in the one dimensional case would appear as line segments

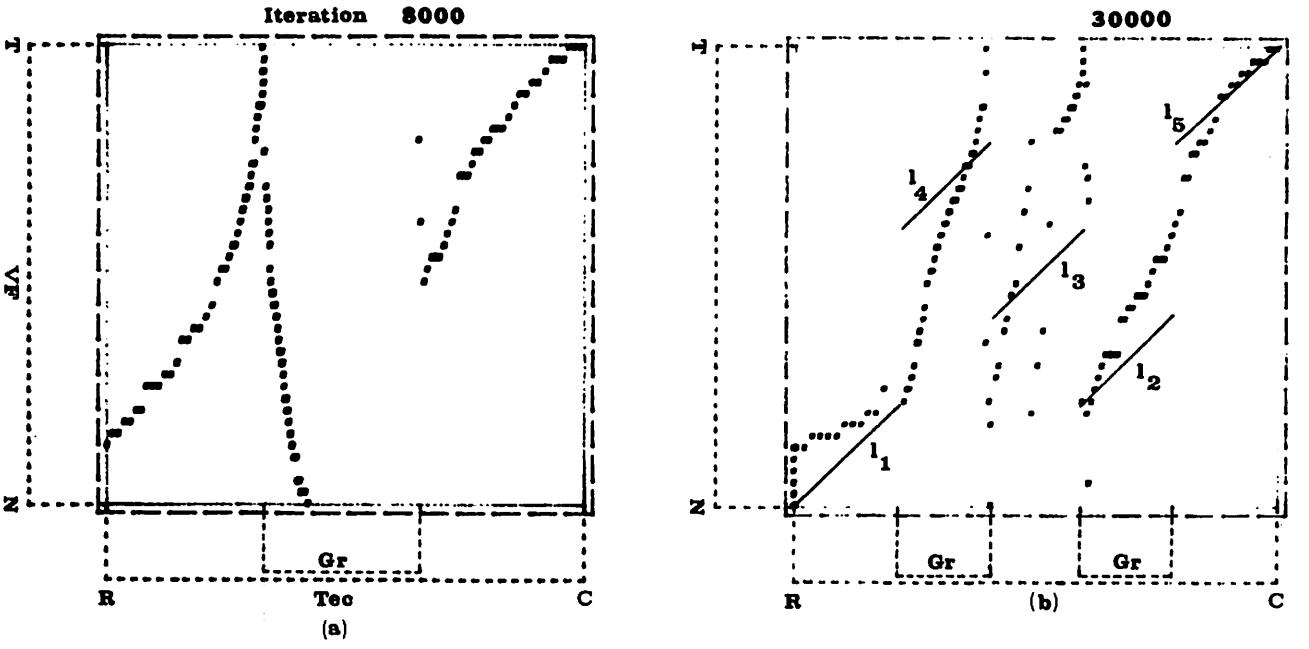

Figure 18. (a) XBAM simulation results of full retina projecting onto a tectum with one graft excised and inverted.

(b) XBAM results of a full retina mapping onto a tectum with two grafts translocated.

l_1 through l_5. BAM produced a completely normal mapping (Overton and Arbib, 1982). XBAM produces behavior closer to that observed experimentally. The disorder in the map is the result of conflicting information from the surface and neighbour interactions. Behavior more closely resembling the ideal case could be produced by appropriately adjusting the weighting constants in equations (10) and (11) of Appendix B.

Experiment VII.

This experiment is designed to compare the behavior of the XBAM simulation with the physiological results obtained during development. The retinal and tectal cell sheets grow at different rates and with different geometries. The retina tends to develop from the center outward in all directions at a uniform rate. The first section of the tectum to develop is the rostrocaudal section. Growth occurs primarily in the caudal and lateral direction. Figure 20 illustrates physiological results produced by Gaze (1974).

Figure 20

The figure contains mappings of the projection of the visual field at various larval stages. There are two interesting features in the data. First, the projection is ordered and initially covers only part of the tectal surface. As the organism continues to develop, the projection expands to fill the entire tectal surface. Second, the projection of the temporal visual field is quite large in comparison to to those of the medial and nasal field. Only after all of the tectal space has been filled does the projection begin to adjust to its normal proportions.

Figure 21a-g contains the XBAM simulation results. In this case, the retina is "grown" from the center outwards. The branches of two fibers are added every 200 iterations. In all cases, the branches of the new fibers are randomly distributed

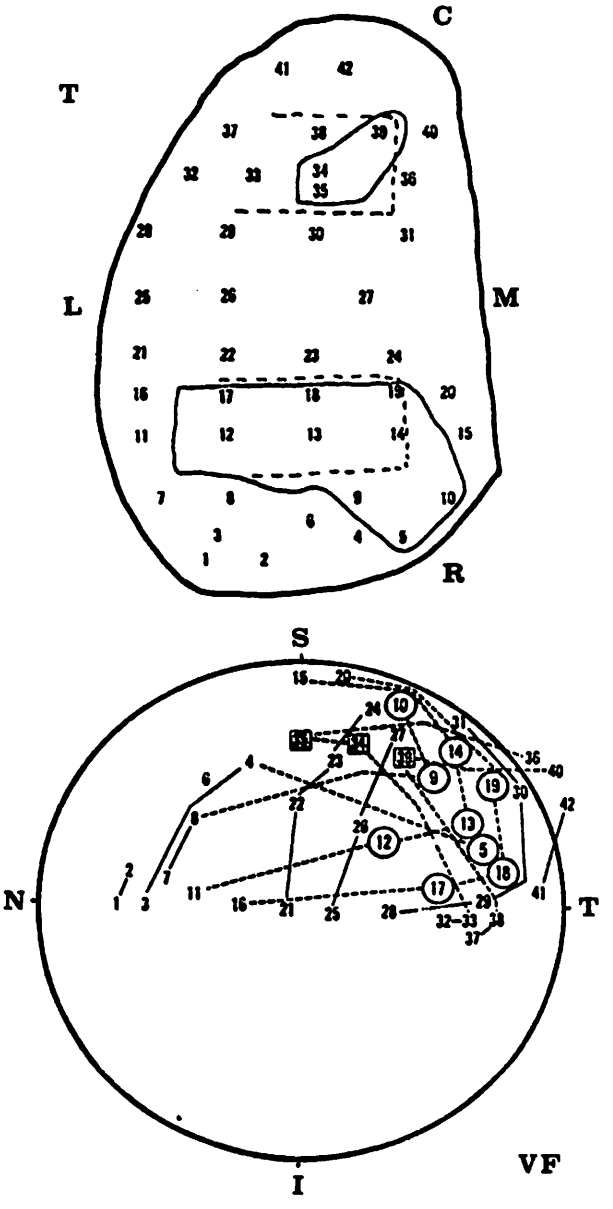

Figure 19. Mapping data from an animal with the positions but not orientations changed for two grafts (Hope 1976).

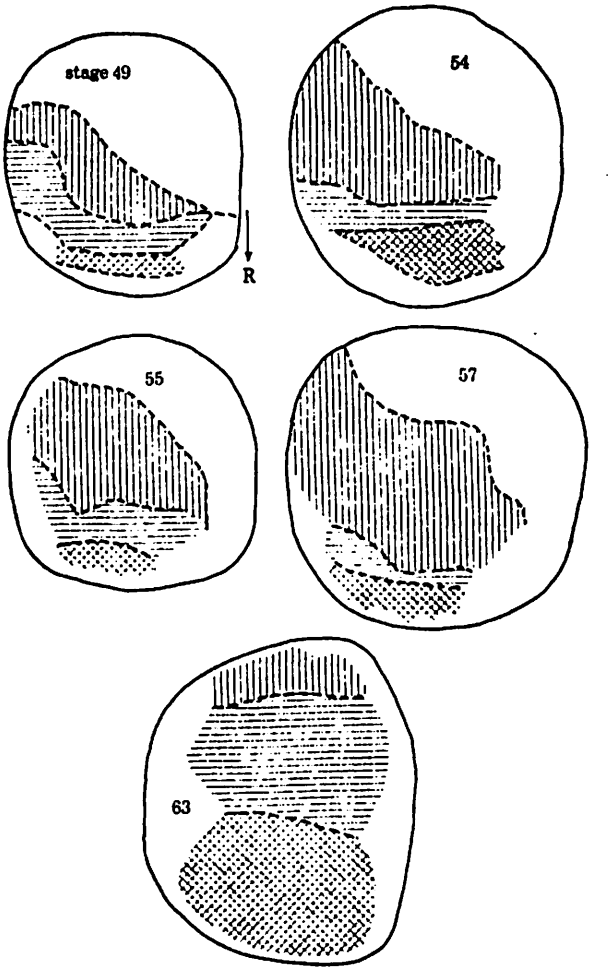

Figure 20. Physiological data of visual field projection mapping during various larval stages (Gaze 1974).

over the tectal surface as delimited in Figure 21a. During the same iteration, the tectal surface is increased in size. The rate of growth in the caudal direction is three times that in the rostral direction. Notice that the middle of the projection onto the tectum is organized as early as iteration 600, cf. Figure 21b, with only 8 fibers represented. As fibers are added from the edges of the retina, the projection remains organized. The tight packing and steep angle seen in the center of the projection indicates that the projection of the medial section of the visual field is compressed as seen in the physiological data. A distinctive "S" shape is evident in the mapping after iteration 2400, Figure 21e. The tails of the projection curve since they cover proportionally more of the tectal surface than does the center. In Figure 21g the branches of the fibers near the center of the projection are tightly packed while the branches of the fibers near the ends are spead out. It should also be noted that the projection is slowly moving in a caudal direction. Continued iteration of the simulation would result in a shift of the mapping in the caudal direction until a mapping projection uniformly covers the entire tectal surface as in Figure 6.

Figure 21

IV. Discussion.

The systems matching theory of the process by which the retino-tectal mapping is produced in lower vertebrates has been discussed. In this light, we presented the Branch-Arrow Model, BAM, as an extension to the Arrow Model of Hope et al. BAM is continuous in nature and includes a generalized neighborhood interaction mechanism as well as explicit boundary interaction. Its behavior was demonstrated through the use of computer simulations. Experiments demonstrate that the systems

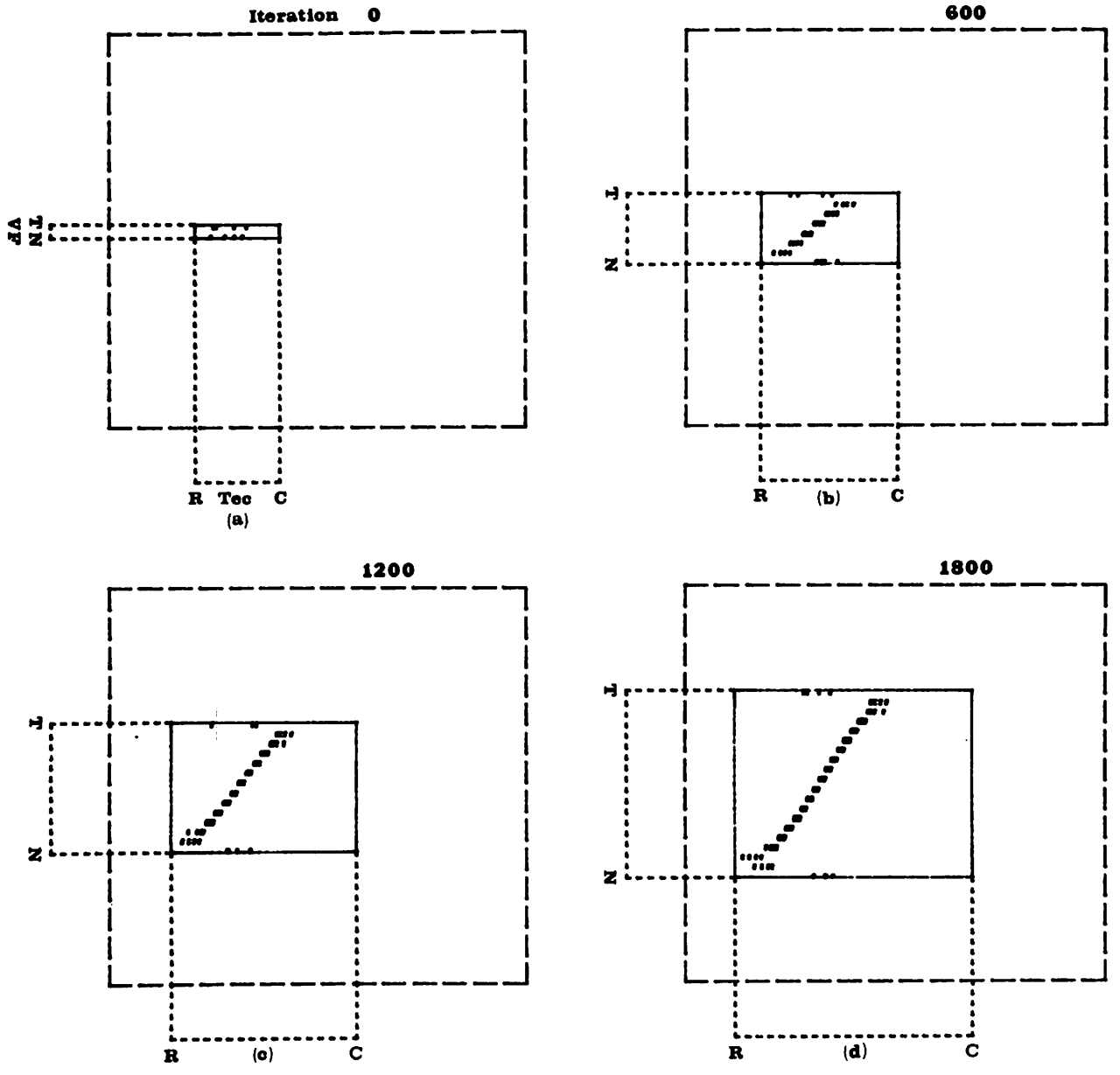

Figure 21, a-d. XBAM simulation of developing visual field and tectum. The visual field grows uniformly out from the center while the tectum grows three times as fast in the caudal direction as in the rostral direction. (a) initial state, (b) 600 iterations, (c) 1200 iterations, (d) 1800 iterations.

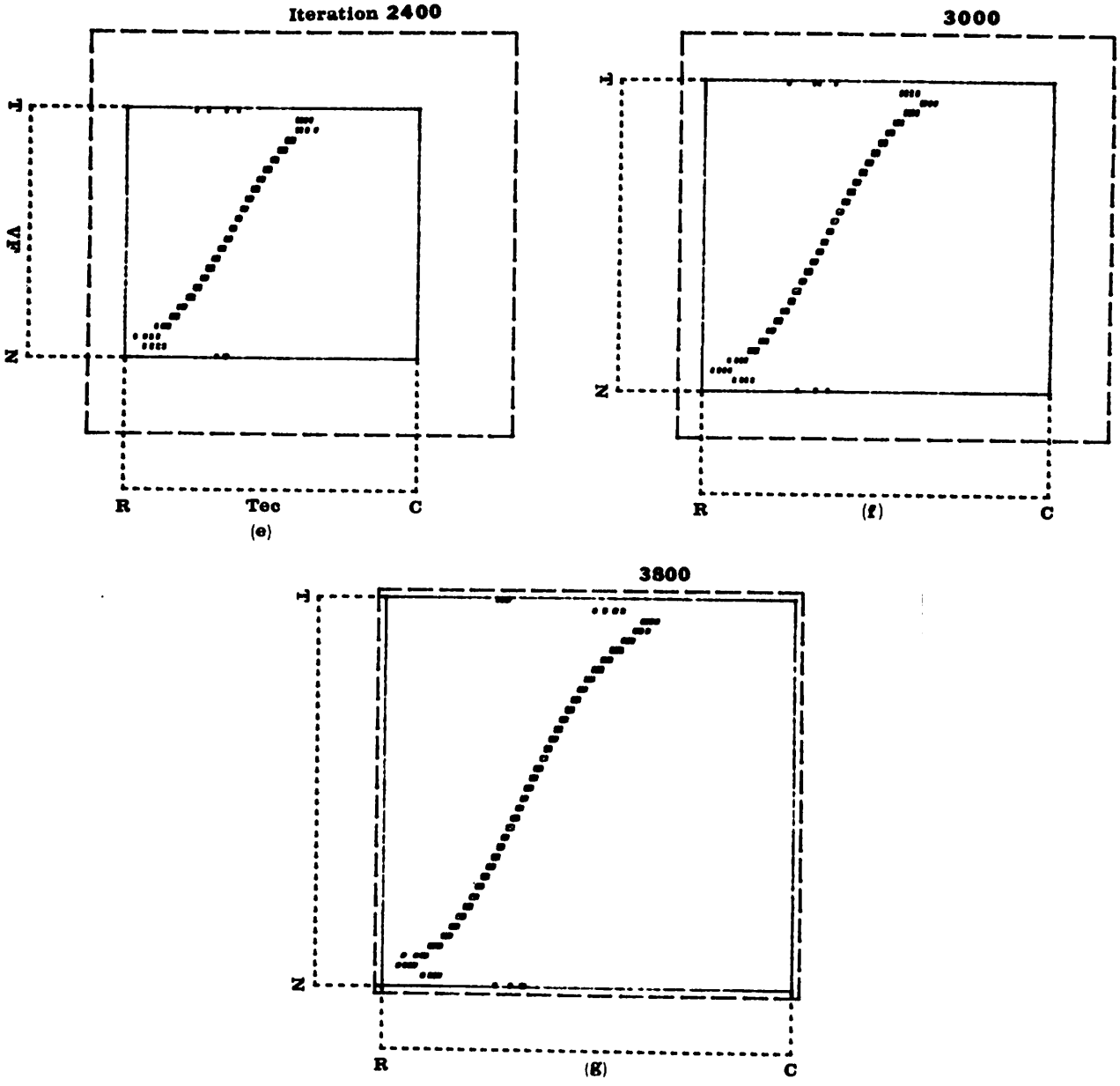

Figure 21, e-g. XBAM simulation of developing visual field and tectum. (e) 2400 iterations, (f) 3000 iterations, (g) 3800 iterations.

matching approach utilizing effective communication between any two retinal cells can account for the majority of the physiological experimental results. However, if the retinal distance allowing communication is reduced to a fraction of the total retinal expanse, the behavior degrades considerably. This suggests that neighborhood interaction mechanisms alone lack sufficient information to produce global organization.

The Marker Induction Model of Willshaw and von der Malsburg can produce behavior similar to the experimental results but requires a degree of initial organization in order to produce a final map which is globally continuous. While this requirement may not be unreasonable, the more general question of the amount of information, or specificity, required by a model to explain the physiological results remains. The Extended Branch-Arrow Model, XBAM, was presented as a compromise between these two approaches.

XBAM combines the local systems matching mechanisms apparent in BAM with a component describing a rough, inaccurate global positioning mechanism derived from the chemoaffinity theory. The behavior of this hybrid model was investigated through computer simulation and was shown to be in good agreement with the physiological data.

The design of (X)BAM reflects the physical structure of the system. Details such as axonal arborization, boundary interaction, and multiple fiber interactions have been included to increase the realism of the model. Expressing our model in a form amenable to computer simulation required the explicit definition of a number of parameters, e.g. the interaction field radius. It has been determined through empirical observation that the model is robust in regard to the settings of these various parameter values. It is not our intent that the actual parameter settings used for our simulations be taken as the quantities on which the validity of our model rests but rather that the model be considered as a possible conceptual

mechanism through which the retino-tectal connections can be organized.

In particular, the values of the parameters were chosen simply to make their relative magnitudes believable. Experimentally determined values for the radius of interaction, average number of branches per retinal fiber, the effect of tectal and graft boundaries, and the ease with which fiber branches can move across surgically induced discontinuities could add a great deal to the model. Our simulations showed that during the course of organization, the density of fiber branch terminations along a graft boundary increased as the boundary became more difficult to cross. A detailed physiological study of the fiber densities seen along graft boundaries in animals could be very useful in evaluating this aspect of model behavior.

The simulation results presented in this paper are one-dimensional in nature. Limited simulations of the two-dimensional analog were conducted. However, they were limited in number and size due to the amount of computation required. The increase in computation was on the order of 100 fold, thus making the use of two-dimensional simulation as a research tool premature. While most of the two-dimensional behavior of a given model can be deduced from the one-dimensional version, certain interesting behavior trends did appear during the time course of organization on our few two-dimensional simulations.

In the one-dimensional experiment involving a rotated graft, some branches were found to remain at the graft boundary due to the conflicting influence felt by the branches on either side: one set inside and the other outside the graft. In the two-dimensional case, branches can again be trapped along a graft boundary. This trapping, however, occurs along one dimension with organizing influence felt along the other dimension. This results in the branches traversing the perimeter of a graft in order to move to the portion of the tectal surface to which they belong instead of crossing the grafted portion. Physiological data indicating the paths across the tectum taken by fibers projecting to different areas would be of great

value in determining the validity of the observed simulation behavior.

A second behavioral anomaly observed in the two-dimensional simulation concerned the shape of the fiber projection fields. Recall that we defined the projection field as the area of the tectum influenced or covered by the branches of a fiber. In the one-dimensional case, we can only conclude that the branches of a particular fiber are grouped together with a uniform overlap in their fields and that the entire surface exhibits reasonably uniform coverage. In the two-dimensional simulation of a normal retina projecting onto a normal tectum, the branches are grouped in such a way as to cover a circular area. The fields are arranged so as to fit the branches in the smallest possible tectal area, given a particular allowable amount of overlap. Again the distribution was such that all of the tectal surface was uniformly covered. When a section of the tectum was excised and rotated, the resulting branch terminations were still grouped, although the shape of the grouping appeared elliptical rather than spherical. The major axis of the set of terminations was in the direction of the rotation of the graft. This suggests the need for physiological experimentation to determine the shape of the area covered by the set of branch terminations for a given fiber. Any differences seen under the conditions of a normal mapping and one with a rotated graft could be compared with the behavior predicted by the simulation.

A final point for discussion concerns the mechanism by which one fiber "knows" how it relates to another. This paper presents a conceptual model which assumes that this information is available to the fibers but does not propose a model of the availability. Several mechanisms have been suggested such as correlation of discharge and chemical gradient (Willshaw and von der Malsburg). The restriction on the distance between two fibers allowing effective communication could be modelled by the latter approach in a rather straightforward manner. If the extent of the indiviual gradients was greatly reduced, then it would be possible for two fibers

which are separated by a distance on the retina large with respect to the extent of the gradients to be marked by different sets of substances. This would result in a lack of information defining the relationship of the somas of the fibers. Physiological work needs to be conducted to determine the types and extents of any position markers on the retina and tectum. In addition, new mechanisms must be sought and further experimental evidence gained if the process by which organizational information is exchanged is to be understood.

Bibliography

Cook, J.E. & Horder, T.J. 1974 Interactions between optic fibers in their regeneration to specitic sites in the goldfish tectum. J. Physiol. 241, 89-90P.

Feldman, J.D., Keating, M.J., & Gaze, R.M. 1975 Retino-tectal mismatch: a serendipitous experimental result. Nature, Lond., 253, 445-446.

Gaze, R.M., Jacobson, M., & Szekely, G. 1963 The retino-tectal projection in Xenopus with compound eyes. J. Physiol., 165, 484-499.

Gaze, R.M., Jacobson, M., & Szeleky, G. 1965 On the formation of connections by compound eyes in Xenopus. J. Physiol., 176, 409-417.

Gaze, R.M. & Sharma, S.C. 1970 Axial differences in the reinnervation of the goldfish optic tectum by regenerating optic fibers. Expl. Brain Res. 10, 171-181.

Gaze, R.M. & Keating, M.J. 1972 The visual system and "neuronal specificity". Nature 237, 375-378.

Gaze, R.M., Keating, M.J., & Chung, S.H. 1974 The evolution of the retinaotectal map during development in Xenopus. Proc. R.Soc. Lond. 185, 301-330.

Hope, R.A., Hammond, B.J., & Gaze, F.R.S. 1976 The arrow model: retinotectal specificity and map formation in the goldfish visual system. Proc. R. Soc. Lond. 194, 447-466.

Horder, T.J. 1971 Retention by fish optic nerve fibers regenerating to new terminal sites on the tectum, "chemospecific" affinity for their original sites. J. Physiol. Lond. 216, 53-55.

Horder, T.J. & Martin, K.A.C. 1977 Translocation of optic fibers in the tectum map be determined by their stability relative to surrounding fiber terminals. J. Physiol., Lond., 271, 23-24P.

Humphery, M.F. and Beazley, L.D. 1981 An electrophysiological study of early patterns of the retinotectal projection during optic nerve regeneration in Hyla Moorei. submitted to Brain Research.

Hunt, R.K. & Jacobson, M. 1973 Development of neuronal locus specificity in Xenopus retinal ganglion cells after surgical transection or after fusion of whole eyes. Dev. Biol., 40, 1-15.

Jacobson, M. & Gaze, R.M. 1965 Selection of appropriate tectal connections by regenerating optic nerve fibers in adult goldfish. Exp. Neurol., 13, 418-430.

Levine, R. & Jacobson, M. 1974 Development of optic nerve fibers is determined by positional markers in the frog tectum. Exp. Neurol. 43, 527-538.

Maturana, H.R., Lettvin, J.Y., McCulloch, W.S., & Pitts, W.H. 1959 Evidence that the cut optic nerve fibers in a frog regenerate to their proper places in the tectum. Science, 130, 1709-1710.

Overton, K.J. & Arbib, M.A. 1982 Systems matching and topographic maps: The branch-arrow model (BAM). In: Competition and Cooperation in Neural Nets (S. Amari and M.A. Arbib, Eds.), Lecture Notes in Biomathematics, Springer-Verlag.

Schmidt, J.T. 1978 Expansion of the half retinal projection to the tectum of in goldfish: an electrophysiological and anatomical study. J. comp. Neurol. 177, 257-278.

Schmidt, J.T. 1978 Retinal fibers alter tectal positional markers during the expansion of the half retinal projection in goldfish. J. comp. Neurol. 177, 279-300.

Schmidt, J.T. & Easter, S.S. 1978 Independant biaxial reorganization of the retinotectal projection: a reassessment. Exp. Brain Res. 31, 155-162.

Sharma, S.C. 1972 Redistribution of visual projections in altered optic tecta of adult goldfish. Proc. Nat. Acad. Sci. U.S.A. 69, 2637-2639.

Sharma, S.C. & Romeskie, M. 1977 Immediate 'compression'of the retinal projection to a tectum devoid of degenerating debris, Brain Res. 134, 367-370.

Sperry, R.W. 1943 Visuomotor coordination in the newt (Triturus viridescens) after regeneration of the optic nerve. J. Comp. Neurol., 79, 33-55.

Sperry, R.W. 1944 Optic nerve regeneration with return of vision in Anurans. J. Neurophysiol. 7, 57-70.

Sperry, R.W. 1945 Restoration of vision after crossing of optic nerves and after contralateral transplantaion of eye. J. Neurophysiol. 8, 15-28.

Sperry, R.M. 1963 Chemoaffinity in the orderly growth of nerve patterns and connections. Proc. Natl. Acad. Sci., U.S.A. 50, 701-709.

Willshaw, D.J. & von der Malsburg, C. 1979 A marker induction mechanism for the establishment of Ordered neural mappings: its application to the retinotectal problem. Phil. Trans. Proc. R. Soc. Lond. B, 287, 203-243.

Udin, S.B. 1977 Rearrangements of the retinotectal projection in Rana Pipiens after unilateral caudal half-tectum ablation. J. comp. Neurol. 173, 561-582.

Yoon, M.G. 1973 Retention of the original toopgraphic polarity by the 180 degree rotated tectal reimplant in young goldfish. J. Physiol. 233, 575-588.

Yoon, M.G. 1975 Readjustment of retinotectal projection following reimplantation of a rotated or inverted tectal tissue in adult goldfish. J. Physiol. 252, 137-158.

Yoon, M.G. 1976 Progress of topographic regulation of the visual projection in the halved optic tectum of adult goldfish. J. Physiol. 257, 621-643.

APPENDIX A

Arrow Model Interchange Rules

One iteration of switching interaction applies the following interchange rule to each retinal fiber, T_k. One of the eight sites immediately adjacent to the present tectal site of T_k (see Figure A.1a) is chosen at random until one containing another fiber, T_n, is found. It should be noted that the boundaries of the tectum are only implicitly considered in that a termination site on a boundary has only five neighbors. The retinal locations, R_k and R_n, of the somas from which fibers T_k and T_n, respectively, emanate are compared and the following process is used to determine the new grid location of the termination of the fibers (Figure A.1b).

* Construct a line, L_t, on the tectum which passes through the site of termination of fiber T_k and is orthogonal to the line connecting the termination sites of both fibers, T_k and T_n.

* Construct a line, L_r, on the retina which passes through the retinal position, R_k, of the soma of fiber T_k and is orthogonal to the line passing through the retinal locations of both fibers, R_k and R_n (Figure A.1b).

* With the superior-inferior retinal axis mapped onto the medial-lateral tectal axis and the nasal-temporal retinal axis mapped onto the rostral-caudal tectal axis, switching is determined as follows: if T_n resides on the same side of line L_t as R_n does with respect to line L_r, then T_k and T_n retain their original locations, otherwise they switch positions.

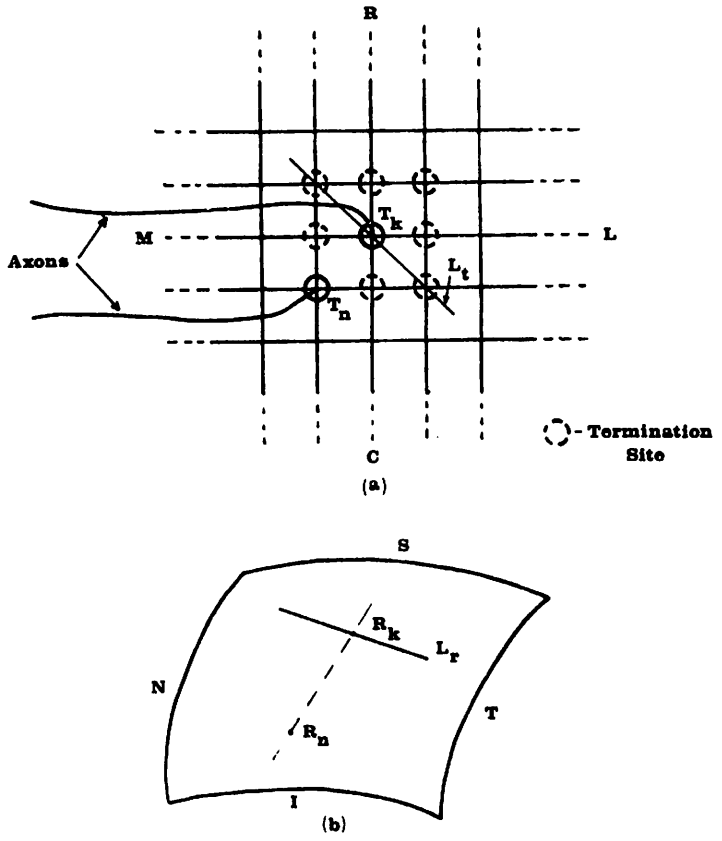

Figure A.1. (a) The grid configuration used in the Arrow Model.

(b) Retinal locations R_k and R_n of the somas of fibres terminating at tectal sites T_k and T_n. R - Rostral, C - Caudal, M - Medial, L - Lateral, N - Nasal, T - Temporal, S - Superior, I - Inferior.

APPENDIX B

Mathematical Specification of BAM

The BAM updating process is obtained by averaging three components: the interaction influence, $\vec{I}_b$, the boundary effect, $\vec{E}_b$, and the average influence, $\vec{A}_b$. The interaction influence component, $\vec{I}_b$, is a continuous analogue of the Arrow-Model interaction process, employed at the level of the branches of a fiber combined with a term describing the local interactions between the branches and the boundaries of the tectum and the various grafts. The average of the physical influence, $\vec{A}_b$, felt by all of the branches of a given fiber is calculated. The ultimate movement of a particular branch is then determined as the weighted sum of these influences.

$$\vec{M}_b = a_1\vec{I}_b + a_2\vec{E}_b + a_3\vec{A}_b \tag{1}$$

where a_1, a_2, and a_3 are weighting constants, $\vec{I}_b$ and $\vec{E}_b$ are described in equations (3) and (4) below, and the average influence is given by

$$\vec{A}_b = \frac{1}{m} \sum_{k \in F_b} (a_4\vec{I}_k + a_5\vec{E}_k) \tag{2}$$

where the sumation ranges over the set F_b of all branches k from the same retinal fiber as b, m is the number of branches in F_b, and a_4, a_5 are weighting constants.

The first term in the physical influence component provides the extension of the Arrow Model. In the Arrow Model, only one of a fiber's eight immediate neighbors is involved during each iteration of its updating. As a result, the fiber in question receives no influence from any of the other neighbouring fibers, nor

from any of the fibers which do not occupy immediately adjacent sites. In BAM, the continuous nature of the tectal surface, the fact that each fiber has a set of branches, and the circle of interaction for each branch eliminate these restrictions. Due to the continuous nature of the tectal surface, the updating process is truly a neighbourhood interaction rather than an interchange. During each iteration, a branch interacts with all other branches whose circles of interaction have a non-empty intersection with the circle of the branch in question to produce the interaction component, $\vec{I}_b$.

To see the shape of this interaction, let B_b be the set of fiber-branches whose interaction circles intersect that of branch b. Let $\vec{U}(b,k)$ be the unit vector in the "interchange direction" for the current position of b and that of k. Then the movement of b induced by its interaction with k is

$$W_d(b,k)\ W_g(b,k)\ \vec{U}(b,k)$$

where the weights W_d (due to the distance of separation) and W_g (due to interaction across a boundary) are described below in equations (4) and (5). Thus the total interaction component is given by

$$\vec{I}_b = \sum_{k \epsilon B_b} W_d(b,k)\ W_g(b,k)\ \vec{U}(b,k) \qquad (3)$$

In the Arrow Model, the interchange of two fibers occurs in discrete steps. When it has been determined that two branches are oriented in the reverse of their retinal locations, they simply exchange positions. In BAM, the influence between two branches, W_d, is graduated depending upon separation. The weight is linear in nature with a value of 1 when the two branches terminate at the same point and 0 when the branches are separated by a distance of twice the radius of their circles of interaction:

$$W_d(b,k) = \begin{cases} 1 - \frac{d(b,k)}{2r} & \text{if } d(b,k) < 2r \\ 0 & \text{otherwise} \end{cases} \quad (4)$$

where r is the radius of interaction on the tectum and d(b,k) denotes the distance between the tectal terminations of fibers b and k.

The weight due to intervening graft boundaries, W_g, is intended to model the discontinuous nature of such edges. Since the edges of grafts are actual surgical disruptions of the surface, wee feel that communication across a graft edge should be attenuated. This is expressed mathematically by including a mulplicative constant for each boundary between the two branches, so that two branches separated by a boundary exhibit less influence on one another than do two branches separated by a similar distance but with no intervening boundaries.

$$W_g(b,k) = a_g^n \quad (5)$$

where a_g is the mulplicative constant determining cross-boundary communication effectiveness, $0 \leq a \leq 1$, and n is the number of graft boundaries intersecting the line segment connecting the terminations of branches b and k.

The simple Arrow Model does not include the boundary of the tectum nor the edges of the grafts as influencing factors. The second term of equation (1) includes this factor explicitly as $\vec{E}_b$.

$$\vec{E}_b = \sum_{q \in Q} W_d(b,q)\ W_g(b,q)\ \vec{U}(b,q) \quad (6)$$

where Q is the index set of all tectal and graft boundaries; $\vec{U}(b,q)$ is the unit vector along the line perpendicular to boundary q and passing through the

termination of branch b; W_d is the weight due to the distance of separation; and W_g is the weight due to graft boundaries.

Tectal and graft edges are physical discontinuities in the surface of the tectum. It should, therefore, be more difficult for an axon to migrate across such a boundary than to move across an unobstructed surface. The boundaries thus have influence by restricting the movements of the branches. As in the case of interacting branches, the magnitude of the influence, W_d, is proportional to the distance from the center of the branch circle to the boundary along a line perpendicular to the boundary.

$$W_d(b,q) = \begin{cases} 1 - \frac{d(b,q)}{r} & \text{if } d(b,q) < r \\ 0 & \text{otherwise} \end{cases} \tag{7}$$

where r is the radius of interaction on the tectum and d(b,q) denotes the distance between the termination of branch b on the tectum and boundary q. In addition, due to the physically discontinuous nature of a boundary, the influence of one branch on another across a boundary is decreased, via W_g. Mathematically, the influence due to boundary interaction felt by branch k is given in (5). The direction of the influence, $\vec{U}$, is always away from the boundary along a line perpendicular to the boundary through the point of termination of the branch in question.

The actual influence, $\vec{M}_b$, used to update the position of a branch b during an iteration is determined as the weighted sum of the physical influences $\vec{I}_b$ and $\vec{E}_b$ felt by the branch and the average $\vec{A}_b$ of the physical influences of the branches from the same fiber, as we saw in equation (1). Since, by definition, the branches of a fiber are connected to one another, we feel that this form of information transfer can take place.

APPENDIX C

Mathematical Specificiation of XBAM

The XBAM physical infuence component consists of three factors. The first two are exactly the neighborhood interaction and boundary influences defined in BAM, see Appendix B. The final factor, $\vec{S}_b$, provides the degree of global information required to account for the translocation experiments. This factor describes the interaction between the branches and the tectal surface. As in BAM, these components are combined with the average influence felt by all of the branches of a fiber to form the total influence felt by each branch during a given iteration,

$$\vec{S}_b = W_s(M(P_r(b),P_t(b)))\,\vec{U}_s(P_r(b),P_t(b)) \qquad (8)$$

where the weight W_s (due to difference of the markers) is described below in equation (9); $P_r(b)$ is an encoding of the retinal position of the soma of the cell emitting branch b; $P_t(b)$ is an encoding of the tectal position of branch b corresponding to the encoding P_r; $M(p,q)$ is a measure of the difference between the retinal and tectal positions; and $\vec{U}_s$ is the unit vector from the branch's current position to its desired final position.

A fiber interacts with the surface of the tectum by way of its branches. Each branch of a fiber is thought to be marked in some manner according to the retinal position of its soma. The marker need not be an indicator of its exact position but rather a marker encoding its general location, e.g. the position should be accurate to within plus or minus the distance allowing effective retinal communication. That is, the marker here is to be considered in the sense of a general position indicator

as opposed to a point to point chemoaffinity. The tectal surface is also posited to be labelled in a similar manner. Each of the branches sample the marker on the tectal surface. The surface influence contains a weight, W_s, which is proportional to the difference between the retinal and tectal labels.

$$W_s(M(a,b)) = \begin{cases} 1 & \text{if } M(a,b) > t_2 \\ \dfrac{M(a,b)-t_1}{t_2 - t_1} & \text{if } t_1 \leq M(a,b) \leq t_2 \\ 0 & \text{otherwise} \end{cases} \tag{9}$$

where t_1 and t_2 are thresholds which determine the interval on the retina allowing effective communication.

The average of the influences, $\vec{A}_b$, felt by the branches of a particular fiber is given by

$$\vec{A}_b = \frac{1}{m} \sum_{k \epsilon F_b} (a_7 \vec{I}_k + a_8 \vec{E}_k + a_9 \vec{S}_k) \tag{10}$$

where the sumation ranges over the set F_b of all branches k from the same retinal fiber as b, m is the number of branches in F_b, and a_7, a_8, and a_9 are weighting constants.

The updating processes used in the Extended Branch-Arrow Model consists of four components. For each of the branches, the interaction influence, boundary influence, surface influence, and the average influence components are combined in a weighted average to form the movement of the branch.

$$\vec{M}_b = a_{10} \vec{I}_b + a_{11} \vec{E}_b + a_{12} \vec{S}_b + a_{13} \vec{A}_b \tag{11}$$

where the a's are weighting constants.